Performance Bounds for an OFDM-Based Joint Radar and Communications System

John R. Krier, Marissa C. Norko, Jeremy T. Reed,* Robert J. Baxley,*
Aaron D. Lanterman, Xiaoli Ma, and John R. Barry
School of Electrical and Computer Engineering, *Georgia Tech Research Institute
Georgia Institute of Technology, Atlanta, GA

***Abstract*—We investigate a joint radar and communications performance bound for a single pair of bistatic transmit and receive antennas that uses orthogonal frequency-division multiplexing (OFDM) transmission. The OFDM transmission signal is designed to simultaneously meet radar target detection and communications signal recovery objectives using training and information symbols on different subcarriers. Given a frequency-selective Rayleigh-distributed fading channel, equally powered and equally spaced training symbols across the occupied bandwidth minimize the mean-square error of the channel estimate, which is tied to a lower bound on ergodic channel capacity. We perform a hypothesis test on the resulting channel estimate to detect and locate targets. We examine the performance region of capacity versus probability of detection in an example scenario in which a single stationary target is present.**

I. Introduction

As spectral congestion increases, efficient spectrum usage becomes increasingly important. In many cases, radar and communication systems operate in different locations, at different times, or in different frequency bands to avoid interference. When the two systems overlap, the performance in each system is impaired due to interference.

The simplest method for radar and communication systems to co-exist is to pre-allocate each system into non-overlapping frequency bands. These bands can be assigned statically (e.g. FCC allocation) or through dynamic spectrum access techniques [1]. When the frequency bands overlap, the systems need to be designed to avoid or mitigate interference. Methods such as interference mitigation [2], interference alignment [3] [4], and waveform design [5] [6] can facilitate coexistence of radar and communication systems. However, these approaches do not share the spectrum to provide mutual benefit. Instead, the available degrees of freedom of time, space, and frequency are mapped as a one-to-one assignment or used to provide interference cancellation. Potentially, better performance is achievable if degrees of freedom are shared. For example, passive radar utilizes transmissions of opportunity (e.g., communication signals) to detect and track targets [7]. However, the radar performance is suboptimal in two ways. First, because there is no sharing, the radar must estimate the intended communications signal. Second, the radar has no control over the transmission. Alternatively, with control of both the radar and communication functions, a system can be co-designed to optimize the performance of the joint system. Such joint systems have been examined in the case where the radar has complete knowledge of the communication signal [8] [9]. However, sharing does not have to be an all or none proposition, and bounds are therefore needed that can describe different degrees of sharing.

This paper presents a joint-performance bound for a co-designed radar and communication system, based on orthogonal frequency-division multiplexing (OFDM), when the transmitted signal contains both a training signal known to the transmitter and receiver and a data signal known only by the transmitter. Communication systems often use training symbols, like pilots, to estimate the channel at the receiver to enhance message decoding. Similarly, a bistatic radar transmitter sends a signal that is known by the receiver through the channel so that the receiver can detect and locate targets. Our approach links the performance of both systems to the fidelity of the channel estimate in order to benchmark waveforms that meet both a data transfer objective and a sensing objective.

The rest of the paper is organized as follows. Section II outlines the channel model and assumptions. In Section III, the relationship between radar target detection and channel estimation is described. The power-constrained joint capacity versus probability of target detection bound is developed in Section IV. Section V details a simulation of a communication and single-target detection system. A summary of the results and directions for future work are presented in Section VI.

Throughout this paper, bold lower-case letters represent vectors and bold upper-case letters represent matrices. $\mathbf{A}^\top$ ($\mathbf{A}^H$) denotes the transpose (Hermitian) of a matrix $\mathbf{A}$. $\mathbf{I}_P$ represents a PxP identity matrix.

II. System Model

Consider a single transmitter and receiver pair, for which the discrete-time baseband equivalent model for the received signal in a "block" is

$$y[k] = \sum_{l=0}^{L-1} h[l]x[k-l] + w[k], \tag{1}$$

978-1-5090-0073-9/15/$31.00 ©2015 IEEE

where $w[k] \sim \mathcal{CN}(0, \sigma_w^2)$ is additive white Gaussian noise, $x[k]$ is the transmitted signal, and $h[k]$ is the channel impulse response, which is known to have L significant taps. We adopt the block-fading assumption that the channel $h[k]$ is constant for the duration of the block, and is independent from one block to the next. We also assume that each channel tap is the summation of clutter and targets, $h[k] = c[k] + s[k]$, where $c[k]$ and $s[k]$ are the contributions of clutter and targets to the channel taps, respectively. Each clutter tap is a zero-mean complex Gaussian random variable with variance $\sigma^2_{c_{[k]}}$, and the clutter taps are independent of one another, the noise, and the target. We also assume a Swerling I point target [10] that is independent of the clutter and noise, so $s[k] = \alpha\delta(k-l)$, where l is the delay bin corresponding to the location of the target and $\alpha \sim \mathcal{CN}\left(0, \sigma_\alpha^2\right)$.

To address inter-block interference, we employ a cyclic prefix, which is a common choice for OFDM schemes [11]. The non-prefix part of the transmitted signal, represented as $\mathbf{x} = [x[0], x[1], \ldots, x[N-1]]^\top$, with $N > L$ carriers, is the superposition of an information bearing signal $\tilde{\mathbf{d}} \in \mathbb{C}^M$ and a training signal that is known to the receiver, $\tilde{\mathbf{b}} \in \mathbb{C}^L$:

$$\mathbf{x} = \mathbf{A}\tilde{\mathbf{d}} + \bar{\mathbf{A}}\tilde{\mathbf{b}}, \tag{2}$$

where $\mathbf{A}$ is an $N \times M$ matrix consisting of a subset of M columns of the N-point ($N = M + L$) IDFT matrix and $\bar{\mathbf{A}}$ is an $N \times L$ matrix consisting of the subset of the L columns of the N-point IDFT matrix that are distinct from $\mathbf{A}$. The actual transmitted signal for a block is longer than N, since it is prefixed by a copy of the final elements of $\mathbf{x}$. But this prefix is removed at the receiver, resulting in the following model for one block of the received signal:

$$\begin{aligned} \mathbf{y} &= \mathbf{H}\mathbf{x} + \mathbf{w} \\ &= \mathbf{H}\mathbf{A}\tilde{\mathbf{d}} + \mathbf{H}\bar{\mathbf{A}}\tilde{\mathbf{b}} + \mathbf{w} \\ &= \mathbf{H}\mathbf{A}\tilde{\mathbf{d}} + \mathbf{B}\mathbf{h} + \mathbf{w}, \end{aligned} \tag{3}$$

where $\mathbf{H}$ is an $N \times N$ circulant matrix whose first column is $[h[0], h[1], \ldots, h[L-1], 0, \ldots, 0]^\top$, $\mathbf{B}$ is an $N \times L$ matrix that contains the first L columns of a circulant matrix whose first column is $\mathbf{b} = \bar{\mathbf{A}}\tilde{\mathbf{b}}$, and $\mathbf{w} = [w[0], w[1], \ldots, w[N-1]]^\top$. The last equality in (3) arises from the commutativity of circular convolution ($\mathbf{H}\mathbf{b} = \mathbf{B}\mathbf{h}$). We assume that the vector of information symbols, $\tilde{\mathbf{d}}$, is zero-mean, circularly-symmetric complex Gaussian with covariance $\mathbf{R}_{\tilde{\mathbf{d}}}$.

The rationale behind placing the data and pilot carriers on different carriers is to reduce complexity. In general, estimating the channel and transmitted data is a non-linear estimation problem whose solution is difficult [11] [12]. Choosing the training and data signals such that channel estimation is decoupled from symbol detection allows for a linear class of estimators for both the channel and the data. In [11], it is shown that one way to achieve this decoupling given our assumed channel model and the use of the OFDM with a cyclic prefix is to constrain $\mathbf{b}$ such that $\mathbf{B}$ has full rank and $\mathbf{B}^H\mathbf{H}\mathbf{A} = \mathbf{0}$ for all $\mathbf{H}$ and $\mathbf{A}$. Also, [11] shows that one way to achieve these constraints on $\mathbf{B}$ is to load the data symbols on the subcarriers that are distinct from the L subcarriers that contain the training symbols. Further, [13] shows that the mean-squared error (MSE) of the linear minimum MSE (LMMSE) channel estimate is minimized only if the pilots are allocated to subcarriers that are equally powered and equally spaced with integer spacing $J = N/L$. The next two sections demonstrate that the channel estimate can be used to detect targets, providing radar functionality, and that both the probability of detection and the lower bound on ergodic channel capacity is a function of the ratio of power between the information symbols and the pilot signals.

III. Hypothesis Testing

To facilitate a linear radar detection scheme, we only use the portion of the received signal due to training signal; i.e., the portion of the signal known to the transmitter. Consider the structure of $\mathbf{y}$ in the case where no information symbols are present; this can be modeled by temporarily setting $\mathbf{A} = \mathbf{0}$. The resulting hypothesis test compares the null hypothesis, $\mathcal{H}_0'$, where the received signal contains returns from clutter and noise and the alternative hypothesis, $\mathcal{H}_1'$, where the received signal consists of returns from the target, clutter, and noise:

$$\mathcal{H}_0' : \ \mathbf{y} = \mathbf{B}\mathbf{c} + \mathbf{w}, \tag{4}$$

$$\mathcal{H}_1' : \ \mathbf{y} = \mathbf{B}(\mathbf{c} + \mathbf{s}) + \mathbf{w}. \tag{5}$$

We use primes to differentiate these hypotheses formed on the data from hypotheses formed on channel estimates, which will be explored in the remaining sections of this paper. Under both hypothesis, $\mathbf{y}$ is the sum of zero-mean, circularly-symmetric complex Gaussian random vectors, and is therefore also a zero-mean, circularly-symmetric complex Gaussian random vector. Letting $\mathbf{\Sigma_c} = \mathrm{E}\{\mathbf{c}\mathbf{c}^H\}$, and $\mathbf{\Sigma_s} = \mathrm{E}\{\mathbf{s}\mathbf{s}^H\}$ be the covariance matrices for clutter and the target, respectively, the covariance matrices for $\mathbf{y}$ under $\mathcal{H}_0'$ and $\mathcal{H}_1'$ are, respectively,

$$\mathrm{E}\{\mathbf{y}\mathbf{y}^H | \mathcal{H}_0'\} = \overbrace{\mathbf{B}\mathbf{\Sigma_c}\mathbf{B}^H + \sigma_w^2\mathbf{I}}^{\mathbf{C}_0} \tag{6}$$

and

$$\begin{aligned} \mathrm{E}\{\mathbf{y}\mathbf{y}^H | \mathcal{H}_1'\} &= \mathbf{B}\mathbf{\Sigma_s}\mathbf{B}^H + \mathbf{B}\mathbf{\Sigma_c}\mathbf{B}^H + \sigma_w^2\mathbf{I} \\ &= \underbrace{\mathbf{B}\mathbf{\Sigma_s}\mathbf{B}^H}_{\mathbf{C}_s} + \mathbf{C}_0. \end{aligned} \tag{7}$$

The Neyman-Pearson (NP) detector decides $\mathcal{H}_1'$ if the likelihood ratio test (LRT) exceeds a threshold

$$\gamma < \frac{p(\mathbf{y} \mid \mathcal{H}_1')}{p(\mathbf{y} \mid \mathcal{H}_0')} = \frac{\frac{1}{\pi^N \det(\mathbf{C}_s + \mathbf{C}_0)} \exp\left(-\mathbf{y}^H \left(\mathbf{C}_s + \mathbf{C}_0\right)^{-1} \mathbf{y}\right)}{\frac{1}{\pi^N \det(\mathbf{C}_0)} \exp\left(-\mathbf{y}^H \mathbf{C}_0^{-1} \mathbf{y}\right)}. \tag{8}$$

Taking the logarithm, incorporating the non-data-dependent terms into the threshold, and using the matrix inversion lemma

results in the final form of the test statistic, which contains a prewhitening filter followed by an estimator-correlator [14]:

$$T_{\mathbf{y}}(\mathbf{y}) = \mathbf{y}^H \mathbf{C}_0^{-1} \mathbf{C}_s \left(\mathbf{C}_s + \mathbf{C}_0\right)^{-1} \mathbf{y}. \tag{9}$$

Some insight into the joint communication/radar problem is gained by considering tests applied to linear estimates of the channel instead of the original data $\mathbf{y}$. Consider linear estimates of the form

$$\hat{\mathbf{h}} = \mathbf{G}\mathbf{B}^H \mathbf{y}, \tag{10}$$

where $\mathbf{G}$ is a Hermitian positive-definite matrix. The $\mathbf{A} = \mathbf{0}$ assumption made earlier in this section may now be relaxed, since the $\mathbf{B}^H\mathbf{H}\mathbf{A} = \mathbf{0}$ property effectively removes the information symbols from consideration. We will show that such an $\hat{\mathbf{h}}$ is a sufficient statistic for our detection problem; the transformation in (10) imparts no loss of information relative to using the original data under the assumption that only the pilot signals are being exploited for detection. (Higher performance might be gained by using the information-bearing part of the data as well; however, such a detector would be more complicated. We leave this as an avenue for future work.)

Testing directly on the channel estimate results in the following hypotheses:

$$\begin{aligned} \mathcal{H}_0 &: \hat{\mathbf{h}} = \mathbf{G}\mathbf{B}^H \mathbf{y} = \mathbf{G}\mathbf{B}^H \left(\mathbf{B}\mathbf{c} + \mathbf{w}\right), \\ \mathcal{H}_1 &: \hat{\mathbf{h}} = \mathbf{G}\mathbf{B}^H \mathbf{y} = \mathbf{G}\mathbf{B}^H \left(\mathbf{B}(\mathbf{c} + \mathbf{s}) + \mathbf{w}\right). \end{aligned} \tag{11}$$

The distributions of $\hat{\mathbf{h}}$ under both these hypothesis are also zero-mean, circularly-symmetric complex Gaussian with covariance matrices[2]

$$\mathrm{E}\{\hat{\mathbf{h}}\hat{\mathbf{h}}^H | \mathcal{H}_0\} = \overbrace{\mathbf{G}\mathbf{B}^H\mathbf{B}\mathbf{\Sigma}_\mathbf{c}\mathbf{B}^H\mathbf{B}\mathbf{G} + \sigma_w^2\mathbf{G}\mathbf{B}^H\mathbf{B}\mathbf{G}}^{\hat{\mathbf{C}}_0} \tag{12}$$

and

$$\begin{aligned} \mathrm{E}\{\hat{\mathbf{h}}\hat{\mathbf{h}}^H | \mathcal{H}_1\} &= \mathbf{G}\mathbf{B}^H\mathbf{B}\mathbf{\Sigma}_\mathbf{s}\mathbf{B}^H\mathbf{B}\mathbf{G} + \mathbf{G}\mathbf{B}^H\mathbf{B}\mathbf{\Sigma}_\mathbf{c}\mathbf{B}^H\mathbf{B}\mathbf{G} \\ &\quad + \sigma_w^2\mathbf{G}\mathbf{B}^H\mathbf{B}\mathbf{G} \\ &= \underbrace{\mathbf{G}\mathbf{B}^H\mathbf{B}\mathbf{\Sigma}_\mathbf{s}\mathbf{B}^H\mathbf{B}\mathbf{G}}_{\hat{\mathbf{C}}_s} + \hat{\mathbf{C}}_0. \end{aligned} \tag{13}$$

We also note that

$$\hat{\mathbf{C}}_0 = \mathbf{G}\mathbf{B}^H\mathbf{C}_0\mathbf{B}\mathbf{G} \text{ and } \hat{\mathbf{C}}_s = \mathbf{G}\mathbf{B}^H\mathbf{C}_s\mathbf{B}\mathbf{G}. \tag{14}$$

Instead of testing the LRT with regards to the raw received data $\mathbf{y}$, we now test the estimate, $\hat{\mathbf{h}}$:

$$\gamma \lessgtr \frac{p(\hat{\mathbf{h}} \mid \mathcal{H}_1)}{p(\hat{\mathbf{h}} \mid \mathcal{H}_0)} = \frac{\frac{1}{\pi^{\mathcal{L}}\det\left(\hat{\mathbf{C}}_s + \hat{\mathbf{C}}_0\right)} \exp\left(-\hat{\mathbf{h}}^H \left(\hat{\mathbf{C}}_s + \hat{\mathbf{C}}_0\right)^{-1} \hat{\mathbf{h}}\right)}{\frac{1}{\pi^{\mathcal{L}}\det\left(\hat{\mathbf{C}}_0\right)} \exp\left(-\hat{\mathbf{h}}^H \hat{\mathbf{C}}_0^{-1} \hat{\mathbf{h}}\right)}, \tag{15}$$

[2]Although the "hat" on $\hat{\mathbf{h}}$ indicates an estimate of $\mathbf{h}$, $\hat{\mathbf{C}}_0$ should not be thought of as an estimate of $\hat{\mathbf{C}}_0$. The "hats" on the covariance matrices indicate covariances associated with $\hat{\mathbf{h}}$ instead of $\mathbf{y}$.

where $\mathcal{L}$ is the length of $\hat{\mathbf{h}}$, which is dependent on the specific channel model. The resulting test statistic on the channel estimate is

$$T_{\hat{\mathbf{h}}}\left(\hat{\mathbf{h}}\right) = \hat{\mathbf{h}}^H \hat{\mathbf{C}}_0^{-1} \hat{\mathbf{C}}_s \left(\hat{\mathbf{C}}_s + \hat{\mathbf{C}}_0\right)^{-1} \hat{\mathbf{h}}. \tag{16}$$

Plugging (10) and (14) into (16) yields

$$T_{\hat{\mathbf{h}}}\left(\hat{\mathbf{h}}\right) = \mathbf{y}^H \mathbf{C}_0^{-1} \mathbf{C}_s \left(\mathbf{C}_s + \mathbf{C}_0\right)^{-1} \mathbf{y} = T_{\mathbf{y}}(\mathbf{y}). \tag{17}$$

That is, once the channel estimate is formed, testing on the channel estimate is the same as testing directly on the received signal that is due to the training signal when (1) the data signal is designed to not interfere with the channel estimate and (2) only the portion of the received signal due to training signal is used for channel estimation.

A. LMMSE Estimation

The LMMSE estimator of the channel derived from the pilot signals is found using the Gauss-Markov theorem [13] [15]:

$$\hat{\mathbf{h}} = \underbrace{\frac{1}{\sigma_w^2}\left(\mathbf{R}_\mathbf{h}^{-1} + \frac{1}{\sigma_w^2}\mathbf{B}^H\mathbf{B}\right)^{-1}}_{\mathbf{G}} \mathbf{B}^H\mathbf{y} = \mathbf{G}\mathbf{B}^H\mathbf{y}, \tag{18}$$

where the estimator *presumes* that $\mathbf{h}$ is zero-mean and $\mathrm{E}\{\mathbf{h}\mathbf{h}^H\} = \mathbf{R}_\mathbf{h}$. The covariance matrix of the error vector, $\epsilon_\mathbf{h} = \hat{\mathbf{h}} - \mathbf{h}$, is

$$\mathbf{R}_\epsilon = \left(\mathbf{R}_\mathbf{h}^{-1} + \frac{1}{\sigma_w^2}\mathbf{B}^H\mathbf{B}\right)^{-1}. \tag{19}$$

The trace of $\mathbf{R}_\epsilon$ gives the MSE. Eliminating $\mathbf{R}_\mathbf{h}^{-1}$ in (18) reduces the LMMSE estimate to the least-squares (LS) estimate.

For the purposes of the *radar detection* problem (11), it does not matter whether $\mathbf{G}$ corresponded to an LS or LMMSE estimator, and in the case of the LMMSE estimator, it does not matter whether the $\mathbf{R}_\mathbf{h}$ assumed was "correct" or not. In fact, one could technically use a $\mathbf{G}$ that does not correspond to either of those kinds of estimators. The only aspect of $\mathbf{G}$ relevant to detection was that it be full rank and Hermitian; combining this with a full rank $\mathbf{B}$ resulted in $\hat{\mathbf{h}}$ being a sufficient statistic for the detection problem.

The analysis in the above paragraph allowed us to be vague about the choice of $\mathbf{R}_\mathbf{h}$ in the LMMSE estimator when considering detection. From the standpoint of *channel estimation*, we could refine our estimate of $\hat{\mathbf{h}}$ using the result of the detection problem to choose the "correct" $\mathbf{R}_\mathbf{h}$, selecting $\mathbf{R}_\mathbf{h} = \mathbf{\Sigma}_\mathbf{c}$ if the null hypothesis was selected and $\mathbf{R}_\mathbf{h} = \mathbf{\Sigma}_\mathbf{c} + \mathbf{\Sigma}_\mathbf{s}$ if the alternative hypothesis was selected. In practice, this subtlety makes little difference in the results of the capacity calculations later described in (23), so in the remainder of this paper, we will generally include only clutter in the $\mathbf{R}_\mathbf{h}$ matrices used in computing capacity bound. There may be instances where a high radar cross section (RCS) target appears that briefly acts as a reflector and helps a communication system, but in general, it is clutter that contributes the most significant multipath energy, and most practical coding schemes will be based on that assumption.

One caveat is that (19) presumes that the random parameters being estimated are generated using the same covariance matrix assumed in the creation of the LMMSE estimator. If the $\mathbf{R_h}$ employed by reality does not match the $\mathbf{R_h}$ used in the model – for instance, if a clutter-only model is used when there is actually a target present – the actual error structure may differ. A detailed study of such mismatches and their impact is left an avenue for future work.

Framing the hypothesis test on channel estimation highlights the equivalence of performing channel estimation and target detection. We highlight similarities in the processing steps (i.e., pulse compression) that occur during channel estimation when it is decoupled from symbol decoding.

IV. Performance Bounds

Let the total transmit power, excluding the cyclic prefix, be $\|\mathbf{x}\|^2 = \Pi$ and define the power in the pilot and data signals to be, respectively,

$$\begin{aligned} \Pi_p &= (1-\rho)\,\Pi, \\ \Pi_d &= \rho\Pi, \end{aligned} \tag{20}$$

where $0 \leq \rho \leq 1$. Using the condition of equally spaced and equally powered pilots [11] stated in Section II,

$$\mathbf{B}^H\mathbf{B} = \Pi_p\mathbf{I}. \tag{21}$$

Using (21) and the assumption that the channel taps are independent (i.e., $\mathbf{R_h}$ is diagonal), the trace of (19) is $\sigma^2_{\Delta h} = \sum_n \sigma^2_{\epsilon_{\mathbf{h}[n]}}$, where

$$\sigma^2_{\epsilon_{\mathbf{h}}[n]} = \frac{\sigma^2_{h[n]}\sigma^2_w}{\sigma^2_w + \Pi_p\sigma^2_{h[n]}}, \quad n = \{0,1,\ldots,L-1\} \tag{22}$$

and $\sigma^2_{h[n]} = \sigma^2_{c[n]}$ is the *assumed* channel variance for $h[n]$ [13].

Given the power and bandwidth constraints, a lower bound on average channel capacity is [13]

$$C \geq \frac{1}{\bar{N}} \sum_{i\in\mathcal{I}_d} E\left[\log\left(1 + \frac{\left|\hat{H}(W^i)\right|^2}{E\left[\left|\tilde{H}(W^i)\right|^2\right] + \frac{M\sigma^2_w}{\Pi_d}}\right)\right], \tag{23}$$

where $\bar{N} = N + L$, $\mathcal{I}_d$ is the set of data subcarrier indices, $W = \exp(j2\pi/N)$, $\tilde{H}(W^i) = H(W^i) - \hat{H}(W^i)$, and the frequency response of the channel and its estimate are $H(W^i)$ and $\hat{H}(W^i)$, respectively.

To determine the presence of a target in the channel estimate, we conduct a test between the hypotheses in (11), selecting $\mathbf{G} = \mathbf{R}_\epsilon/\sigma^2_w$ as specified in (18) and (19).

Using the assumption of a Swerling I point target, $\mathbf{s} = \alpha\mathbf{e}_l$, where $\mathbf{e}_l$ is an L-length vector that is one at the l^{th} element and zero elsewhere. Therefore, the alternative hypothesis becomes

$$\mathcal{H}_1\text{: } \hat{\mathbf{h}} = \frac{1}{\sigma^2_w}\mathbf{R}_\epsilon\mathbf{B}^H(\mathbf{B}\mathbf{c} + \alpha\mathbf{B}\mathbf{e}_l + \mathbf{w}) \tag{24}$$

for a target assumed to be in range bin l.

Using (21) and independence among the channel taps, the covariance matrices for the channel estimate under H_0 and H_1 are, respectively,

$$\mathbf{\Sigma}_{H_0} = \frac{1}{\sigma^4_w}\mathbf{R}_\epsilon\left(\Pi^2_p\mathbf{\Sigma_c} + \Pi_p\sigma^2_w\mathbf{I}\right)\mathbf{R}_\epsilon \tag{25}$$

and

$$\mathbf{\Sigma}_{H_1} = \frac{1}{\sigma^4_w}\Pi^2_p\sigma^2_\alpha\mathbf{R}_\epsilon\mathbf{e}_l\mathbf{e}_l^H\mathbf{R}_\epsilon + \mathbf{\Sigma}_{H_0}, \tag{26}$$

where (19) has been used. Because the clutter channel taps are independent of one another, $\mathbf{\Sigma_c}$ is a diagonal matrix with elements $\sigma^2_{\mathbf{c}[n]}$, $n = \{0,1,\ldots,L-1\}$. Since we assume the clutter and target are independent, $\mathbf{R}_\epsilon$ is a diagonal matrix with elements given in (22), which results in both $\mathbf{\Sigma}_{H_0}$ and $\mathbf{\Sigma}_{H_1}$ being diagonal.

The first term on the right-hand side of (26) is the covariance matrix, after the MMSE filter, of the received signal that contains a target, and is a matrix of all zeros except the $(l,l)^{\text{th}}$ entry, which is[3]

$$\hat{\sigma}^2_\alpha = \frac{\Pi^2_p\sigma^2_\alpha}{\sigma^4_w}\left(\frac{1}{\sigma^2_{h[l]}} + \frac{\Pi_p}{\sigma^2_w}\right)^{-2}. \tag{27}$$

Therefore,

$$p\left(\hat{\mathbf{h}}|H_0\right) = \prod_{n=0}^{L-1}\mathcal{CN}\left(0,\sigma^2_{H_0[n]}\right) \tag{28}$$

and

$$p\left(\hat{\mathbf{h}}|H_1\right) = \prod_{n=0}^{L-1}\mathcal{CN}\left(0,\sigma^2_{H_1[n]}\right), \tag{29}$$

where

$$\sigma^2_{H_0[n]} = \frac{\Pi^2_p\sigma_{c[n]} + \Pi_p\sigma^2_w}{\sigma^4_w}\left(\frac{1}{\sigma^2_{h[n]}} + \frac{\Pi_p}{\sigma^2_w}\right)^{-2} \tag{30}$$

and

$$\sigma^2_{H_1[n]} = \begin{cases} \sigma^2_{H_0[n]} & n \neq l \\ \hat{\sigma}^2_\alpha + \sigma^2_{H_0[n]} & n = l \end{cases}. \tag{31}$$

Substituting (28)-(31) into the logarithm of (15) results in

$$\begin{aligned} &\ln\left(\sigma^2_{H_0[l]}\right) - \ln\left(\hat{\sigma}^2_\alpha + \sigma^2_{H_0[l]}\right) \\ &- \left|\hat{h}[l]\right|^2\left(\frac{1}{\sigma^2_{H_0[l]}} - \frac{1}{\hat{\sigma}^2_\alpha + \sigma^2_{H_0[l]}}\right) > \ln(\gamma), \end{aligned} \tag{32}$$

which is the same as testing just the l^{th} range bin or channel tap. Moving the non-dependent terms to the right hand side results in the test statistic

$$r\left(\hat{h}[l]\right) = \left|\hat{h}[l]\right|^2 > \gamma', \tag{33}$$

which is a square-law detector [10]. To find the threshold that will result in a desired probability of false alarm, $\mathrm{P_{FA}}$, note that $\hat{h}\,[l]$ is a zero-mean, circularly-symmetric complex Gaussian

[3]The scalar $\hat{\sigma}^2_\alpha$ should not be thought of as an estimate of σ^2_α.

random variable. Therefore, the test statistic under the null hypothesis becomes an exponential distribution:

$$p\left(r\left(\hat{h}[l]\right)\,\middle|\,H_0\right)=\begin{cases}\frac{1}{\sigma^2_{H_0}}\mathrm{e}^{-\frac{r\left(\hat{h}[l]\right)}{\sigma^2_{H_0}}} & r\left(\hat{h}[l]\right)\geq 0\\ 0 & r\left(\hat{h}[l]\right)<0\end{cases}. \quad (34)$$

The $\mathrm{P_{FA}}$ is obtained by integrating

$$\mathrm{P_{FA}}=\int_{\gamma'}^{\infty}\frac{1}{\sigma^2_{H_0}}\mathrm{e}^{\frac{r\left(\hat{h}[l]\right)}{\sigma^2_{H_0}}}\,dr\left(\hat{h}[l]\right), \quad (35)$$

which leads to the threshold

$$\gamma'/\sigma^2_{H_0}=-\ln(\mathrm{P_{FA}}). \quad (36)$$

The probability of detection is derived by integrating the alternative hypothesis distribution above this fixed threshold:

$$\mathrm{P_D}=\int_{\gamma'}^{\infty}\frac{1}{\hat{\sigma}^2_{\alpha}+\sigma^2_{H_0[l]}}\mathrm{e}^{\frac{r\left(\hat{h}[l]\right)}{\hat{\sigma}^2_{\alpha}+\sigma^2_{H_0[l]}}}\,dr\left(\hat{h}[l]\right) \quad (37)$$

$$=\mathrm{e}^{\frac{-\gamma'}{\hat{\sigma}^2_{\alpha}+\sigma_{H_0[l]}}}=\mathrm{P_{FA}}^{\frac{1}{1+\chi_l}}, \quad (38)$$

where χ_l can be viewed as the target signal-to-interference-plus-noise ratio (SINR) after the MMSE filter has been applied to the data. Specifically, using the simplifications resulting from the equi-power and equi-spacing of the pilot signal,

$$\chi_l=\frac{\hat{\sigma}^2_{\alpha}}{\sigma^2_{H_0}}=\frac{\Pi_p\sigma^2_{\alpha}}{\sigma^2_{w}+\Pi_p\sigma^2_{c[l]}}. \quad (39)$$

The fact that testing on the channel estimate leads to a square-law detector on the channel estimate offers insight into how channel estimation and target detection are linked for the class of waveforms considered. Specifically, $\mathbf{B}^H\mathbf{y}=\mathbf{B}^H\mathbf{B}\mathbf{h}+\mathbf{B}^H\mathbf{w}$ projects the N-dimensional received data onto an L-dimensional space. From a radar viewpoint, pre-multiplying the received data by $\mathbf{B}^H$ is equivalent to pulse compressing at the L different delays corresponding to range bins. Due to the diagonal assumption of the channel, the output of $\mathbf{B}^H\mathbf{y}$ is normalized by the power in the transmit signal for the LS estimator. For the LMMSE estimator, the normalization contains the power in the transmit signal and also the prior knowledge about the statistics (i.e., power) in the channel [15]. The channel capacity given in (23) and the probability of detection in (37) are dependent on the power in the pilot signals, which is a function of ρ. Section V shows how varying ρ traces out the achievability region for the joint system.

V. Numerical Results

This section examines a simulation for a bistatic transmitter and receiver pair. The center frequency is 3 GHz, the bandwidth is 8 MHz, and the total transmitter power is varied. Both the transmitter and receiver gains equal 5 dB. As shown in Figure 1, the distance between the transmitter and the receiver is 19 km, the path from the transmitter to the target is 17 km, and the path from the target to the receiver is 17 km. The target is set to an RCS of 40 dBsm, which is comparable to a jet airliner [10]. The clutter is assumed to fall off exponentially

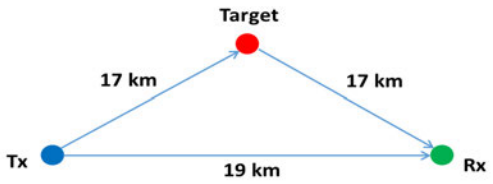

Figure 1. Relative distances between the transmitter, receiver, and the target.

with range, so the variance is $\sigma^2_{c[n]}=A\mathrm{e}^{-T_s n/\tau}$, where $n=\{0,1,\ldots,L-1\}$ and T_s is the sampling rate, τ is the maximum delay spread of the channel, and A is the expected power in the first clutter channel tap. For the simulations presented here, $\tau=3$ μs and $A=0.05G_{LOS}$, where G_{LOS} is the gain that would result from a direct free-space path from the transmitter to the receiver. The number of frequency subcarriers is 8192, with 1024 assigned to pilots and the remaining assigned to the data. In this system, there are no degrees-of-freedom exploitable for mitigating clutter; hence, the maximum SINR (and thus, the maximum probability of detection) is limited by the signal-to-clutter ratio at the range bin where the target is located. Therefore, the range of the target is chosen to be at a distance where the target dominates clutter. Future work may examine channel models and waveforms that allow for clutter mitigation.

System performance is analyzed while the ratio of power between pilot and information symbols is changed while maintaining a fixed total power; i.e., Π is held fixed while ρ is varied between zero and one. Figure 2a shows the channel capacity as the power allocation is varied. The lower bound on channel capacity increases drastically when only a small amount of power is added to the data symbols, but effect of additional data power diminishes rapidly afterwords. The maximum is reached when ρ is 0.8599, 0.8433, and 0.8291 for received SNR per symbols of 25 dB, 35 dB, and 45 dB, respectively. While this does indicate that only a small proportion of power is needed to produce the channel estimate that results in the best lower bound on channel capacity, the performance degrades relatively slowly as more power is allocated to channel estimation. For example, for the 45-dB received SNR case, the lower bound is 5.82 bps/Hz when 90% of the power is used to perform channel estimation, compared to the maximum of 7.31 bps/Hz (i.e., when only 17.09% of the power is used for channel estimation), resulting in a decrease in capacity of only 20.40%. The detection performance when the probability of false alarm is 10^{-5} is shown in Figure 2b, illustrating that detection performance monotonically increases as more power is used to perform channel estimation.

Figure 3 explores the trade-off between data transfer and target detection. Each curve represents the joint performance, for the given received SNR, as ρ is varied between 0 and 1. The curves differ in shape, depending on the of total transmit power. When there is little power (25 dB, solid line) for the joint mission, almost all of the power is needed to obtain any target detection. When there is a large amount of power

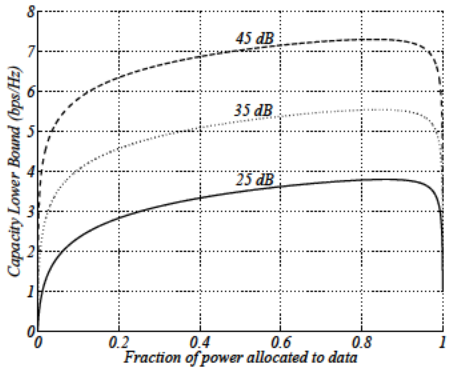

(a) Power allocation vs. capacity lower bound

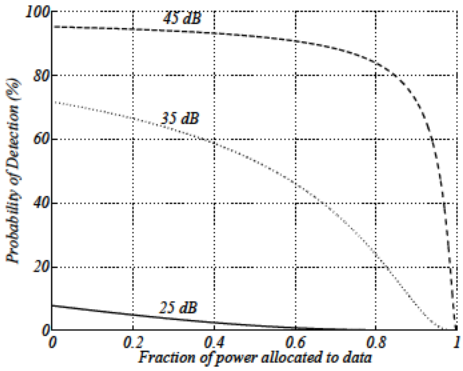

(b) Power allocation vs. probability of detection

Figure 2. Performance of individual system objectives as the power allocation between data and training is varied.

(45 dB, dashed line), there is a mutual benefit to performing channel estimation in that both capacity and the probability of detection increase until probability of detection reaches its maximum value. Further increasing the energy in the pilots does not sufficiently improve the channel estimate to warrant the decrease in energy available for information transfer.

VI. Conclusion

This paper examined a joint radar and communication performance bound for an OFDM transmission that uses pilot symbols that are loaded onto carriers separate from the data. The resulting performance bound ties together a lower bound on ergodic channel capacity and the probability of target detection through the proportion of power in the data signal versus the power in the training signal. The example in this paper demonstrates a case where there is a relatively small drop in the bound on capacity as a higher percentage of the power is allocated to the channel estimation and target detection portion of the signal. In this light, co-designed systems can utilize resources more effectively than two systems operating independently. Future work could expand on this model by examining the impact of other (i.e.,hardware) constraints or allowing information symbols as a source of channel estimation and/or an aid to radar detection.

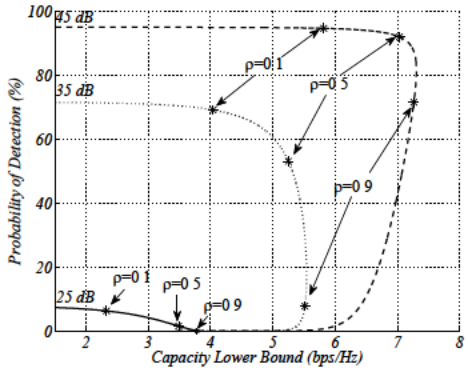

Figure 3. Joint performance bound for capacity and target detection performance. Each curve is created by varying the ratio of power in the target multi-path reflection to the clutter power, or the target SINR defined in (39).

Acknowledgment

This work was supported by the Defense Advanced Research Projects Agency (DARPA) program "Shared Spectrum Access for Radar and Communication." We thank Drs. Richard Causey and Jonathan Odom for their valuable advice.

References

[1] Z. Ji and K. R. Liu, "Cognitive radios for dynamic spectrum access-dynamic spectrum sharing: A game theoretical overview," *IEEE Communications Magazine*, vol. 45, no. 5, pp. 88–94, 2007.

[2] R. Monzingo, *Introduction to adaptive arrays*. Raleigh, NC: SciTech Pub, 2011.

[3] K. Gomadam, V. R. Cadambe, and S. A. Jafar, "A distributed numerical approach to interference alignment and applications to wireless interference networks," *IEEE Transactions on Information Theory*, vol. 57, no. 6, pp. 3309–3322, 2011.

[4] M. Razaviyayn, M. Sanjabi, and Z.-Q. Luo, "Linear transceiver design for interference alignment: Complexity and computation," *IEEE Transactions on Information Theory*, vol. 58, no. 5, pp. 2896–2910, 2012.

[5] S. Sodagari, A. Khawar, T. C. Clancy, and R. McGwier, "A projection based approach for radar and telecommunication systems coexistence," in *Proc. IEEE Global Communications Conference (GLOBECOM)*, 2012, pp. 5010–5014.

[6] S. Amuru, R. M. Buehrer, R. Tandon, and S. Sodagari, "On the coexistence of MIMO radar with communication systems."

[7] W. Melvin and J. Sheer, *Principles of Modern Radar Applications: volume 3 - Radar Applications*. New York, NY: Scitech Pub Inc, 2014.

[8] C. Sturm, T. Zwick, and W. Wiesbeck, "An OFDM system concept for joint radar and communications operations." in *Proc. VTC Spring*, 2009.

[9] M. Braun, C. Sturm, and F. K. Jondral, "Maximum likelihood speed and distance estimation for OFDM radar," in *Proc. IEEE Radar Conference*, 2010, pp. 256–261.

[10] M. A. Richards, *Fundamentals of Radar Signal Processing*. Tata McGraw-Hill Education, 2005.

[11] S. Ohno and G. B. Giannakis, "Optimal training and redundant precoding for block transmissions with application to wireless OFDM," *IEEE Transactions on Communications*, vol. 50, no. 12, pp. 2113–2123, 2002.

[12] X. Ma, L. Yang, and G. B. Giannakis, "Optimal training for MIMO frequency-selective fading channels," *IEEE Transactions on Wireless Communications*, vol. 4, no. 2, pp. 453–465, 2005.

[13] S. Ohno and G. B. Giannakis, "Capacity maximizing MMSE-optimal pilots for wireless OFDM over frequency-selective block Rayleigh-fading channels," *IEEE Transactions on Information Theory*, vol. 50, no. 9, pp. 2138–2145, 2004.

[14] S. M. Kay, *Fundamentals of Statistical Signal Processing, Vol. II: Detection Theory*. Prentice-Hall, 1998.

[15] ——, *Fundamentals of Statistical Signal Processing: Estimation Theory*. Prentice-Hall, 1993.